ACS Medicinal Chemistry Letters

Letter

pubs.acs.org/acsmedchemlett

EGFR-Targeted Magnetic Nanovectors Recognize, *in Vivo*, Head and Neck Squamous Cells Carcinoma-Derived Tumors

David Colecchia,[†] Elena Nicolato,[‡] Costanza Ravagli,[⊥] Paola Faraoni,[¶] Angela Strambi,[†] Matteo Rossi,[†,∥] Saer Doumett,[⊥] Elisa Mosconi,[§] Erica Locatelli,[#] Mauro Comes Franchini,[#] Manuela Balzi,[¶] Giovanni Baldi,[⊥] Pasquina Marzola,[*,‡] and Mario Chiariello[*,†]

[†]Consiglio Nazionale delle Ricerche, Istituto di Fisiologia Clinica and Istituto Toscano Tumori-AOU Senese, Core Research Laboratory, Via Fiorentina 1, 53100 Siena, Italy

[‡]Centro Piattaforme Tecnologiche and [§]Dipartimento di Informatica, Università di Verona, Strada Le Grazie 15, 37134 Verona, Italy

[⊥]Dipartimento di Nanobiotecnologie, Colorobbia Consulting-Cericol, Via Pietramarina 53, 50053 Sovigliana Vinci, Italy

[¶]Dipartimento di Scienze Biomediche, Sperimentali e Cliniche "Mario Serio", Università di Firenze, Viale Morgagni 50, 50134 Firenze, Italy

[#]Dipartimento di Chimica Industriale "Toso Montanari", Università di Bologna, Viale Risorgimento 4, 40136 Bologna, Italy

Supporting Information

ABSTRACT: Head and neck squamous cell carcinomas (HNSCC) are a diverse group of tumors with high morbidity and mortality that have remained mostly unchanged over the past decades. The epidermal growth factor receptor (EGFR) is often overexpressed and activated in these tumors and strongly contributes to their pathogenesis. Still, EGFR-targeted therapies such as monoclonal antibodies and kinase inhibitors have demonstrated only limited improvements in the clinical outcome of this disease. Here, we take advantage of the extraordinary affinity of EGF for its cognate receptor to specifically target magnetite-containing nanoparticles to HNSCC cells and mediate, *in vitro*, their cellular upload. On the basis of this, we show efficient accumulation, *in vivo*, of such nanoparticles in subcutaneous xenograft tumor tissues in sufficient amounts to be able to mediate visualization by magnetic resonance imaging. Overall, our EGF-coated nanosystem may warrant, in the near future, novel and very efficient theranostic approaches to HNSCC.

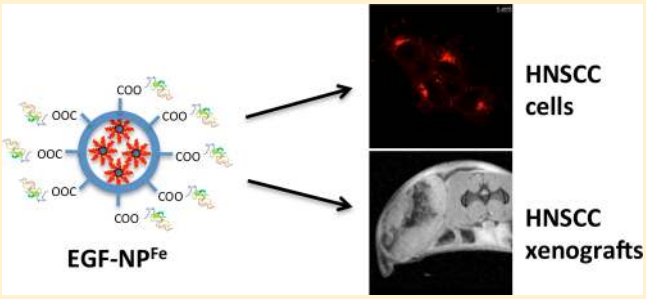

KEYWORDS: *HNSCC, EGFR, nanoparticles, magnetite, targeting delivery systems*

Overall, head and neck cancer accounts for more than 500 000 cases annually worldwide.[1,2] Among them, head and neck squamous cell carcinomas (HNSCC) account for about 90% of all these malignant tumors.[3] They are characterized by local tumor aggressiveness, high rate of early recurrences, metastasis, and development of second primary tumors, which are the major cause of morbidity and mortality.[3] Unfortunately, about two-thirds of patients with HNSCC present with advanced stage disease, commonly involving regional lymph nodes, and treatment decisions are often complicated, involving many specialists, including head and neck surgeons, medical and radiation oncologists, radiologists, plastic surgeons, and dentists.[3] Moreover, although used for decades in HNSCC, conventional therapies (surgery, radiation, or chemoradiation) have several limitations in terms of quality of life or even death of the patients and the estimated five-year survival rate for advanced disease remains poor (30%−40%).[4]

The epidermal growth factor receptor (EGFR) is particularly important in the pathogenesis of HNSCC. Indeed, overexpression of the EGFR gene is seen in about 90% of tumors,[5] and augmented EGFR expression correlates with increased local recurrence and worse overall survival.[6,7] Conversely, few mutations have been observed for this receptor in HNSCC patients.[8]

While EGFR overexpression plays a clear role in HNSCC and FDA has approved the use of cetuximab combined to standard chemo/RT regimens, unfortunately, this specific anti-EGFR monoclonal antibody[9] as well as several tyrosine kinase inhibitors[10] have not shown a significant improvement in clinical outcome to date, possibly due to primary and secondary mechanisms of resistance to EGFR inhibition in these tumors. Nonetheless, taking advantage of the very high expression of EGFR in HNSCC cells[11] to "actively" target these tumors may still represent a successful method to approach this disease for novel diagnostic and therapeutic options. In this context,

Received: July 10, 2017
Accepted: November 7, 2017
Published: November 7, 2017

DOI: 10.1021/acsmedchemlett.7b00278
ACS Med. Chem. Lett. 2017, 8, 1230−1235

nanotechnology has already demonstrated its potential in cancer diagnosis and therapy for the possibility of transporting drugs but also "contrast agents" to cancer locations both passively, by the so-called "enhanced permeability and retention" effect,[12] and actively, taking advantage of specific molecular markers expressed on the cell surface of different tumor cells.[13,14] Introduction onto the surface of nanoparticles (NPs) of targeting agents for specific recognition of these markers will therefore lead to internalization and selective accumulation of the NPs in cell compartments,[15] allowing intracellular release of their content.

Herein, we provide demonstration that biocompatible nanoparticles (NP) can be successfully targeted, *in vitro* and *in vivo*, to HNSCC cells expressing the EGFR, by taking advantage of the very high "natural" affinity of its cognate ligand, EGF, opportunely conjugated on NP's surface. Interestingly, such biocompatible shell contains an inorganic core composed of nanometric magnetite (Fe_3O_4) particles that perform as very efficient contrast agents for magnetic resonance imaging (MRI). Indeed, by using this imaging approach, we demonstrate that, in this configuration (EGF-coated, magnetite-containing, nanoparticles, EGF-NP^{Fe}), our nanosystem is already able to specifically target, *in vivo*, HNSCC-derived tumors, with immediate potential for diagnostic purposes. In perspective, thanks to its tumor specificity, further functionalization of our system with drugs or other therapeutic approaches (e.g., gold nanorods for hyperthermia) may warrant, in the near future, novel and very efficient theranostic approaches for HNSCC treatment.

Magnetite (Fe_3O_4) nanoparticles (NP^{Fe}), synthesized according to a polyol-like method,[16] were first superficially functionalized with a proper organic ligand [N-(3,4-dihydroxyphenethyl) dodecanamide (DDA)] and dispersed in tetrahydrofuran (THF) (see Supporting Information for details). The organic-coated magnetite nanoparticles were dispersed in THF then encapsulated into the polymeric polylactic-*co*-glycolic-*co*-polyethylene glycol (PLGA-*b*-PEG-COOH)[17] matrix, which is Food and Drug Administration (FDA) approved for medical purpose. The process led to the formation of a stable phosphate buffered suspension of hybrid nanoparticles according to the nanoprecipitation technique[18] using a THF to water ratio of 1/10[19−21] (Scheme 1). The so-achieved suspension was dialyzed

Scheme 1. Preparation and Characterization of EGF-NP^{Fe} Nanoparticles

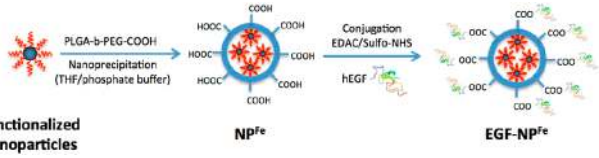

in tangential flow membranes to remove the organic solvent, the impurities, and not-reacted reagents and then concentrated to about 0.3% (w/w) in Fe_3O_4 (150 mL). Finally, the nanoparticles were completely characterized. The mean particle size and mean polydispersity index for NP^{Fe} was determined by dynamic light scattering (DLS) and found to be 50.8 ± 0.6 nm and 0.11 ± 0.01, respectively, indicating a narrow size distribution (see Supporting Information). Transmission electron micrographs (TEM) for NP^{Fe} showed clusters of small numbers of inorganic particles homogeneously dispersed in the polymeric matrix with an average diameter of 50 nm (see Supporting Information). ζ-Potential revealed a negative surface charge, equal to −43.0 ± 0.2 mV, which can be attributed to the presence of several carboxylic acids onto the external surface. The iron content was determined by inductively coupled plasma optical emission spectrometry and found to be equal to 2.7 mg/mL.

Subsequently, human epidermal growth factor (hEGF) was linked to the outer surface (−COOH) of the NP^{Fe} using the typical conjugation with 1-ethyl-3-(3-(dimethylamino)propyl) carbodiimide (EDC) and *N*-hydroxysulfosuccinimide. Briefly, 1-ethyl-3-(3-(dimethylamino)propyl) carbodiimide hydrochloride and *N*-hydroxysulfosuccinimide were added to NP^{Fe} in phosphate-buffered solution, and then a solution of hEGF (0.5 mg/mL, in phosphate buffer) was added.[22] The reaction was carried out at room temperature, and after purification and concentration as reported above, a 7 mL suspension of EGF-NP^{Fe} was obtained (Scheme 1). The iron content was found to be equal to 2.3 mg/mL, indicating only minor losses during the conjugation reaction. Mean particle size was 50.5 ± 1.1 nm, and mean polydispersity index was 0.12 ± 0.01 by DLS analysis (see Supporting Information). Zeta potential measurements post-conjugation reveal the presence of a new peak at −13.4 ± 2.0 mV (see Supporting Information) that can be attributed to the partial disappearance of some carboxylic acid groups, now involved in the amide bond with hEGF, thus confirming the linkage of the hEGF onto the surface. The TEM and STEM analysis confirmed the results of the DLS investigations, showing no alteration of the inner morphological structure of EGF-NP^{Fe} (Suppl. Figure 1A) and a homogeneous distribution of the nanoparticles into the sample (Suppl. Figure 1B).

The amount of hEGF linked to NP^{Fe} was determined by UV−vis analysis using the bicinchoninic acid assay in three samples: EGF-NP^{Fe}; NP^{Fe} without hEGF to evaluate the signal ascribed to analytical interference; and wash waters collected during the purification step. The results showed that the concentration of hEGF in the wash waters was below the detection limit and can therefore be considered negligible, whereas the hEGF was attached to the hybrid nanoparticles at a concentration of 438 μg/mL, giving a weight ratio of hEGF to NP^{Fe} of 0.15.

HNSCC frequently overexpress the EGFR and cancer derived cell lines often maintain this characteristic upon immortalization.[11] Among the different cell lines available, we chose, as model systems for this disease, HN6 and HN13 cells, which express very high levels of the endogenous receptor, even when compared to breast cancer-derived cell lines (Figure 1A).

The ability of EGF-NP^{Fe} to specifically recognize HNSCC is based on the correct interaction between the EGFR (expressed on the cells) and its cognate ligand (exposed on the nanoparticles). To check the correct exposure of the EGF, once immobilized on the NP and, consequently, its ability to interact with and activate its receptor, we monitored the signal transduction pathway downstream of EGFR. Specifically, a key intracellular event, upon EGFR activation, is the increased phosphorylation of the ERK1/2 proteins (Figure 1B). Indeed, treatment of HN13 cells with EGF-NP^{Fe} readily (after 5′ and 15′) stimulated the phosphorylation of ERK1/2 proteins, evaluated by Western blot analysis with specific antiphospho antibodies, at an extent comparable to optimal "free" EGF concentrations (Figure 1C). As an additional control, magnetite-containing nanoparticles, conjugated to a "scrambled" peptide of the same length and amino acid composition of EGF (SCR-NP^{Fe}) failed to induce any ERK1/2 phosphor-

DOI: 10.1021/acsmedchemlett.7b00278
ACS Med. Chem. Lett. 2017, 8, 1230−1235

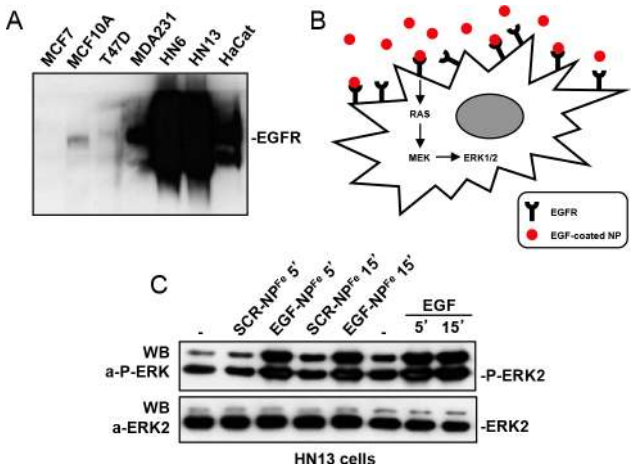

Figure 1. (A) Western blot analysis, using an anti-EGFR antibody, of total cell lysates from breast cancer (MCF7, MCF10A, T47D, and MDA231) and head and neck squamous cell carcinoma (HN6, HN13) cells. HaCat are Human immortalized keratinocytes. (B) Schematic representation of the signaling pathway activated by EGF-NP^{Fe} upon interaction with the specific EGFR on target cells. (C) Measurement of ERK1/2 activation by Western blot analysis of NH13 total cell lysates, using a specific antiphospho-ERK1/2 antibody. An anti-ERK2 antibody was used in the lower panel for normalization purposes.

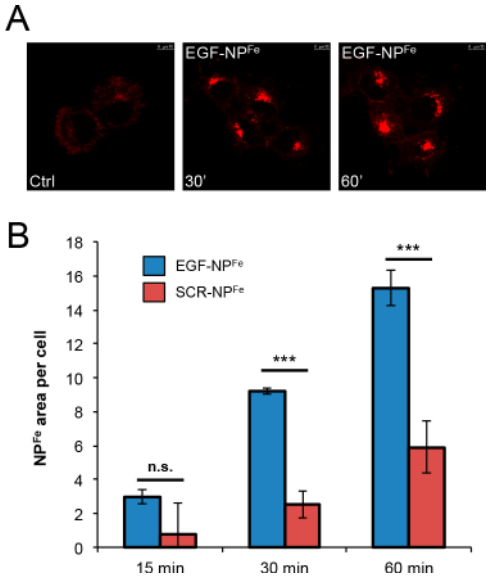

Figure 2. (A) Evaluation of internalization of EGF-NP^{Fe}, in HN13 cells, by confocal microscopy analysis, by using specific anti-EGF antibodies. (B) Evaluation of internalization of SCR-NP^{Fe} and EGF-NP^{Fe}, loaded with DyLight650 fluorophore, by confocal microscopy analysis, in HN13 cells.

ylation, in the same experimental conditions (Figure 1C), suggesting that the EGF functionalization confers the NP^{Fe} the ability to efficiently interact with the EGFR and possibly, to mediate downstream effect, for example, internalization of the ligand−receptor complex.[23] Similar results were also obtained in a different cell line, that is, HeLa cells, expressing the EGFR (Suppl. Figure 2).

The possibility of using EGF-NP^{Fe} for imaging applications strictly depends on its ability not only to recognize the EGFR, but also to accumulate into tumor cells. To address whether NP^{Fe} and their content accumulate in tumor tissues in sufficient amounts for imaging (by appropriate contrast agents) or therapy (by cytotoxic drugs), we next explored EGF-NP^{Fe} internalization, in HNSCC cell cultures, by confocal fluorescence microscopy. First, HN13 cells were incubated for increasing times with freshly prepared EGF-NP^{Fe} and then fixed and stained with anti-EGF antibodies. As shown in Figure 2A, EGF-NP^{Fe} readily accumulated inside HN13 cells upon incubation for 30 min and 1 h, time-points compatible with a very efficient mechanism of active internalization, such as EGF receptor-mediated endocytosis.[23] Conversely, untreated cells (control, Ctrl) showed only a weak background signal, ascribable to the presence of low levels of endogenous EGF produced by these cells.[24] To control for specific cellular internalization of EGFR targeted nanovectors, we next incubated, for increasing times, HN13 cells with SCR-NP^{Fe} and EGF-NP^{Fe}, both loaded with the DyLight650 fluorophore (see Supporting Information) (Figure 2B). Importantly, EGF-NP^{Fe} were internalized into HN13 cells at a rate much faster than SCR-NP^{Fe}, control nanovectors (Figure 2B), supporting the specificity of our approach.

All together, our results therefore support an efficient EGF-dependent mechanism of internalization of nanoparticles inside of EGFR expressing cells, which could allow accumulation of these structures in amount feasibly compatible with successive *in vivo* applications, for example, magnetic resonance imaging (MRI). Therefore, we next sought to investigate whether EGF-NP^{Fe} could efficiently accumulate, *in vivo*, into HNSCC-derived tumors, expressing high endogenous levels of EGFR. In this context, we first investigated, by MR imaging in normal BalbC mice, biodistribution of nanoparticles administered by intravenous (i.v.) injection. It is well-known that the transversal relation rate (1/T2) of tissues is decreased in proportion to the concentration of iron and that quantitative measurement of T2 relaxation time allows determination of the concentration of iron in tissues.[25,26] Considering the high transversal relaxivity of the nanoparticles (Suppl. Figure 3), their biodistribution was evaluated by T2-weighted images (T2w). As shown in Figure 3, we observed a substantial signal drop in the liver, while signal intensity (SI) in muscle remained close to the precontrast values. The SI drop in the liver was clearly detectable during the first 2 h after injection, but it persisted up to 30 days postinjection (see dashed lines in Figure 3, delineating the margins of the right lobe of the liver). SI drop was also detectable in kidneys (see arrow), suggesting that urinary excretion can contribute to the elimination of this nanoparticle. The signal intensity in heart was slightly decreased immediately after administration but recovered to the preinjection value within 120 min.

Ultimately, we decided to use a classical subcutaneous xenograft tumor approach, generated by injecting HNSCC HN6 cells in the flank of athymic nude FOXN1$^{nu/nu}$ mice (Suppl. Figure 4), to test for tumor targeting of EGF-NP^{Fe}. Importantly, the prerequisite for application of iron-based nanoparticles to MRI imaging is the capability of obtaining high concentration of nanoparticles selectively in the tumors tissue. While this is generally reached by direct injection of NPs in tumor tissue, other administration routes, i.v. or intraperitoneal (i.p.), should be highly desirable to noninvasively treat tumors growing in internal organs. When tumor size reached ∼200 mm^3, we therefore performed MRI acquisition before injecting the nanoparticles (Pre) and after i.v. injection of EGF-NP^{Fe} (24 mg/kg), detecting accumulation of EGF-NP^{Fe} 24−48 h after their administration (Figure 4A, see arrows), demonstrating the

DOI: 10.1021/acsmedchemlett.7b00278
ACS Med. Chem. Lett. 2017, 8, 1230−1235

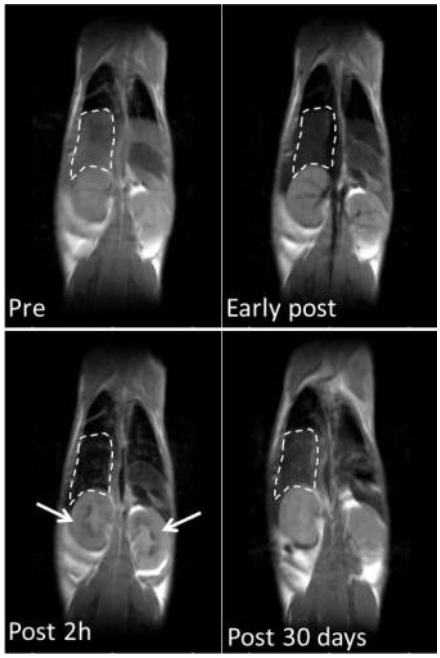

Figure 3. *In vivo* biodistribution. Balb C mice were injected i.v. with NP^{Fe} at a dosage of 6 mg Fe/kg (n = 10) of body weight, at different intervals. Representative T2w images of one animal, acquired prior to and after administration of NP^{Fe}, are shown. Dashed lines delineate the margins of the right lobe of the liver; arrows indicate kidneys.

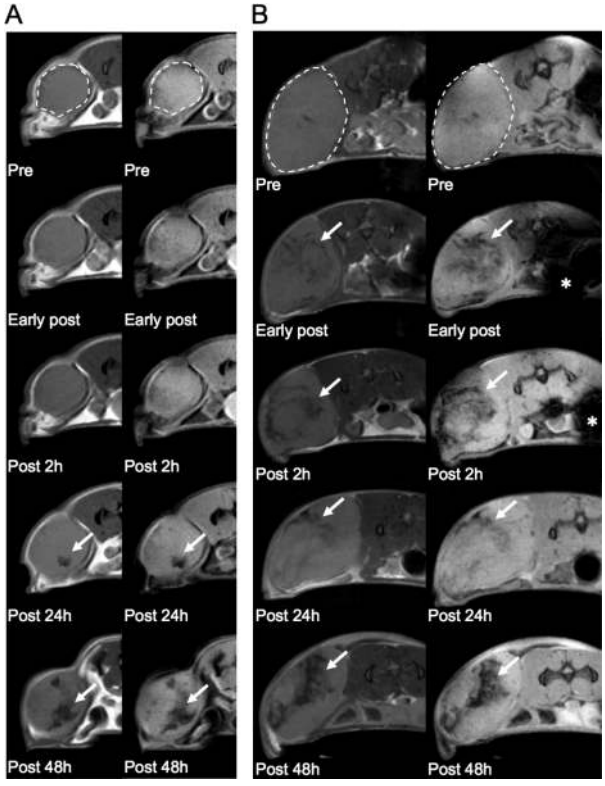

Figure 4. *In vivo* tumor targeting. (A) Representative T2 (left line) and T2*w (right line) images obtained by i.v. injection, in a mouse bearing subcutaneous tumors, and using EGF-NP^{Fe} at 24 mg/kg. Arrows indicate areas of signal drop at long time point after injection. (B) Representative T2 (left line) and T2*w (right line) images obtained by i.p. injection. Dashed lines in pretreatments (Pre) delineate tumor margins. Asterisks show the injection site.

potential of these nanovectors for diagnostic applications. Next, we also tested the i.p. route of administration at the same dosage. Interestingly, much faster accumulation of nanoparticles was obtained upon i.p. administration of EGF-NP^{Fe}, with a faster decrease in SI of some regions of the tumor compared to i.v. injection (Figure 4B). The effect on the SI increased with time and reached its maximum 48 h after injection (Figure 4B). It is noteworthy that, when we injected naked NPs, either i.v. or i.p., the signal drop detectable in tumors was negligible in comparison with EGF-NP^{Fe} (Suppl. Figure 5). As an additional control, when EGF-NP^{Fe} were injected directly into the tumor, we demonstrated lack of local diffusion to neighbor tissues (Suppl. Figure 6), suggesting the possibility of local usage of these NPs for therapeutic application (e.g., by laser-induced hyperthermia) of superficial tumors. In this case, strong decrease of the tumor signal intensity was observed, as expected, in the tumor mass.

Overall, the described results prove the efficacy of our specifically assembled ferrimagnetic nanosystems to interact with EGFR expressing cells through functionalization of NP^{Fe} surface with the EGFR ligand, hEGF. In turn, EGF−EGFR interaction was able to mediate cellular internalization, which may not only allow immediate recognition of tumor cells by NP^{Fe}, but also contribute to restrain them to the tumor for longer times, increasing their concentration and even allowing to follow, by MRI, time-dependent tumor responses to therapies. Indeed, we have clearly shown specific localization of sufficient amounts of EGF-NP^{Fe} to tumors to be imaged, *in vivo*, by MRI. This will be particularly significant, in perspective, for subsequent theranostic approaches, deriving from the potential combination of our diagnostic system with drugs or, for example, plasmonic nanorods for hyperthermia, loaded into the nanovectors (Figure 5), an opportunity that we are

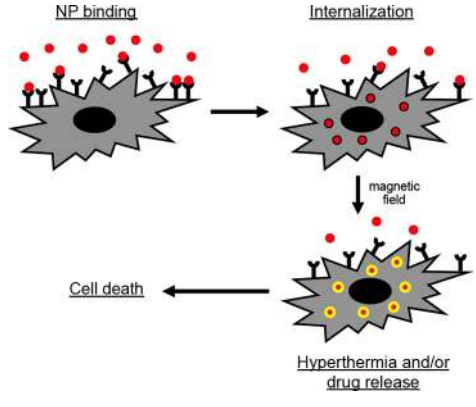

Figure 5. Schematic representation of experimental strategy for potential theranostic approaches.

currently actively investigating. Importantly, we expect that our system, targeting EGFR overexpressing tumors but not based on its inhibition for therapeutic effects, will be only limitedly affected by mechanisms of resistance that, conversely, reduce long-term efficacy of other agents (drugs, antibodies) inhibiting the EGF receptor.

Another potential field of application for our ferrimagnetic nanovectors, to immediately impact on HNSCC patients, could be in the accurate staging of cervical lymph node basins, by taking advantage of lymphatic transport of nanovectors to draining lymph nodes, upon intratumoral injection and their high specificity for accumulation into tumor cells. Indeed,

DOI: 10.1021/acsmedchemlett.7b00278
ACS Med. Chem. Lett. 2017, 8, 1230−1235

presence of cervical lymphatic metastasis is among the most important prognostic factors in HNSCC patients[27] and is essential to develop an appropriate treatment plan, especially in patients with advanced stage tumors that are more likely to present nodal involvement.[28] The current "staging" lymph node techniques indeed include clinical examination, computed tomography (CT) scan, and MRI. The latter, however, although less invasive, is able to detect metastases only with extremely variable sensitivity and specificity (from 36% to 94% and from 50% to 98%, respectively).[29] For this reason, at present, the dissection of the neck with the histological examination of the lymph nodes is still the "gold standard" in the staging of metastases,[30] and therefore, there is a strong need for a non- or minimally invasive procedures able to provide high quality prognostic information that could equal histological test results. On the other hand, in fact, the elective neck dissection, on average, detects lymph node metastases only in 30% of patients and, consequently, in approximately 70% of patients, this operation is not necessary.[31]

■ ASSOCIATED CONTENT

Supporting Information

The Supporting Information is available free of charge on the ACS Publications website at DOI: 10.1021/acsmedchemlett.7b00278.

Full experimental procedures and supplementary figures (PDF)

■ AUTHOR INFORMATION

Corresponding Authors

*E-mail: mario.chiariello@cnr.it.

*E-mail: pasquina.marzola@univr.it.

ORCID

Erica Locatelli: 0000-0002-0711-8082

Mauro Comes Franchini: 0000-0001-5765-7263

Mario Chiariello: 0000-0001-8434-5177

Present Address

[‖]VIB Center for Cancer Biology, 3000 Leuven, Belgium.

Author Contributions

D.C. and E.N. contributed equally to this paper. The manuscript was written through contributions of all authors. All authors have given approval to the final version of the manuscript.

Funding

This work was supported by a grant from Regione Toscana (POR CReO 2007−13).

Notes

The authors declare no competing financial interest.

■ ACKNOWLEDGMENTS

Regione Toscana is acknowledged for funding this project. We thank TLS Foundation in Siena for providing infrastructure and instrumentation.

■ ABBREVIATIONS

NP, nanoparticles; NP^{Fe}, magnetite (Fe_3O_4) nanoparticles; $EGF\text{-}NP^{Fe}$, EGF-coated, magnetite-containing, nanoparticles; HNSCC, head and neck squamous cell carcinomas; EGFR, epidermal growth factor receptor; hEGF, human epidermal growth factor; SCR, scrambled; MRI, magnetic resonance imaging; SI, signal intensity.

■ REFERENCES

(1) Chaturvedi, A. K.; Anderson, W. F.; Lortet-Tieulent, J.; Curado, M. P.; Ferlay, J.; Franceschi, S.; Rosenberg, P. S.; Bray, F.; Gillison, M. L. Worldwide trends in incidence rates for oral cavity and oropharyngeal cancers. *J. Clin. Oncol.* **2013**, *31*, 4550−9.

(2) Jemal, A.; Bray, F.; Center, M. M.; Ferlay, J.; Ward, E.; Forman, D. Global cancer statistics. *Ca-Cancer J. Clin.* **2011**, *61*, 69−90.

(3) Argiris, A.; Karamouzis, M. V.; Raben, D.; Ferris, R. L. Head and neck cancer. *Lancet* **2008**, *371*, 1695−709.

(4) Du, Y.; Peyser, N. D.; Grandis, J. R. Integration of molecular targeted therapy with radiation in head and neck cancer. *Pharmacol. Ther.* **2014**, *142*, 88−98.

(5) Kalyankrishna, S.; Grandis, J. R. Epidermal growth factor receptor biology in head and neck cancer. *J. Clin. Oncol.* **2006**, *24*, 2666−72.

(6) Chung, C. H.; Ely, K.; McGavran, L.; Varella-Garcia, M.; Parker, J.; Parker, N.; Jarrett, C.; Carter, J.; Murphy, B. A.; Netterville, J.; Burkey, B. B.; Sinard, R.; Cmelak, A.; Levy, S.; Yarbrough, W. G.; Slebos, R. J.; Hirsch, F. R. Increased epidermal growth factor receptor gene copy number is associated with poor prognosis in head and neck squamous cell carcinomas. *J. Clin. Oncol.* **2006**, *24*, 4170−6.

(7) Psyrri, A.; Yu, Z.; Weinberger, P. M.; Sasaki, C.; Haffty, B.; Camp, R.; Rimm, D.; Burtness, B. A. Quantitative determination of nuclear and cytoplasmic epidermal growth factor receptor expression in oropharyngeal squamous cell cancer by using automated quantitative analysis. *Clin. Cancer Res.* **2005**, *11*, 5856−62.

(8) Sun, W.; Califano, J. A. Sequencing the head and neck cancer genome: implications for therapy. *Ann. N. Y. Acad. Sci.* **2014**, *1333*, 33−42.

(9) Ang, K. K.; Zhang, Q.; Rosenthal, D. I.; Nguyen-Tan, P. F.; Sherman, E. J.; Weber, R. S.; Galvin, J. M.; Bonner, J. A.; Harris, J.; El-Naggar, A. K.; Gillison, M. L.; Jordan, R. C.; Konski, A. A.; Thorstad, W. L.; Trotti, A.; Beitler, J. J.; Garden, A. S.; Spanos, W. J.; Yom, S. S.; Axelrod, R. S. Randomized phase III trial of concurrent accelerated radiation plus cisplatin with or without cetuximab for stage III to IV head and neck carcinoma: RTOG 0522. *J. Clin. Oncol.* **2014**, *32*, 2940−50.

(10) Worden, F. P.; Sacco, A. G. Molecularly targeted therapy for the treatment of head and neck cancer: a review of the ErbB family inhibitors. *OncoTargets Ther.* **2016**, *9*, 1927−43.

(11) Sriuranpong, V.; Park, J. I.; Amornphimoltham, P.; Patel, V.; Nelkin, B. D.; Gutkind, J. S. Epidermal growth factor receptor-independent constitutive activation of STAT3 in head and neck squamous cell carcinoma is mediated by the autocrine/paracrine stimulation of the interleukin 6/gp130 cytokine system. *Cancer Res.* **2003**, *63*, 2948−56.

(12) Maeda, H. Tumor-selective delivery of macromolecular drugs via the EPR effect: background and future prospects. *Bioconjugate Chem.* **2010**, *21*, 797−802.

(13) Arosio, P.; Orsini, F.; Piras, A. M.; Sandreschi, S.; Chiellini, F.; Corti, M.; Masa, M.; Múčková, M.; Schmidtová, L.; Ravagli, C.; et al. MR imaging and targeting of human breast cancer cells with folate decorated nanoparticles. *RSC Adv.* **2015**, *5*, 39760−39770.

(14) Ramzy, L.; Nasr, M.; Metwally, A. A.; Awad, G. A. S. Cancer nanotheranostics: A review of the role of conjugated ligands for overexpressed receptors. *Eur. J. Pharm. Sci.* **2017**, *104*, 273.

(15) Allen, T. M.; Cullis, P. R. Drug delivery systems: entering the mainstream. *Science* **2004**, *303*, 1818−22.

(16) Psimadas, D.; Baldi, G.; Ravagli, C.; Comes Franchini, M.; Locatelli, E.; Innocenti, C.; Sangregorio, C.; Loudos, G. Comparison of the magnetic, radiolabeling, hyperthermic and biodistribution properties of hybrid nanoparticles bearing CoFe2O4 and Fe3O4 metal cores. *Nanotechnology* **2014**, *25*, 025101.

(17) Locatelli, E.; Franchini, M. C. Biodegradable PLGA-b-PEG polymeric nanoparticles: synthesis, properties, and nanomedical applications as drug delivery system. *J. Nanopart. Res.* **2012**, *14*, 1316.

(18) Schubert, S.; Delaney, J. T., Jr; Schubert, U. S. Nanoprecipitation and nanoformulation of polymers: from history to powerful possibilities beyond poly (lactic acid). *Soft Matter* **2011**, *7*, 1581−1588.

DOI: 10.1021/acsmedchemlett.7b00278
ACS Med. Chem. Lett. 2017, 8, 1230−1235

(19) Baldi, G. *Functionalised Nanoparticles, Their Production and Use*. Italian Patent WO2007/077240, July 12, 2007.
(20) Baldi, G. *Magnetic Nanoparticles for the Application in Hyperthermia, Preparation Thereof and Use in Constructs Having a Pharmacological Application*. Italian Patent WO2008/074804, June 26, 2008.
(21) Baldi, G. *Magnetite in Nanoparticulate Form*. Italian Patent WO2011/073922, June 23, 2011.
(22) Franchini, M. C.; Baldi, G.; Ravagli, C.; Mazzantini, F.; Loudos, G.; Adan, J.; Masa, M.; Psimadas, D.; Fragogeorgi, E. A.; Locatelli, E.; Innocenti, C.; Sangregorio, C. In vivo anticancer evaluation of the hyperthermic efficacy of anti-human epidermal growth factor receptor-targeted PEG-based nanocarrier containing magnetic nanoparticles. *Int. J. Nanomed.* **2014**, *9*, 3037−56.
(23) Carter, R. E.; Sorkin, A. Endocytosis of functional epidermal growth factor receptor-green fluorescent protein chimera. *J. Biol. Chem.* **1998**, *273*, 35000−7.
(24) Yonesaka, K.; Zejnullahu, K.; Lindeman, N.; Homes, A. J.; Jackman, D. M.; Zhao, F.; Rogers, A. M.; Johnson, B. E.; Jänne, P. A. Autocrine production of amphiregulin predicts sensitivity to both gefitinib and cetuximab in EGFR wild-type cancers. *Clin. Cancer Res.* **2008**, *14*, 6963−73.
(25) Masotti, A.; Pitta, A.; Ortaggi, G.; Corti, M.; Innocenti, C.; Lascialfari, A.; Marinone, M.; Marzola, P.; Daducci, A.; Sbarbati, A.; Micotti, E.; Orsini, F.; Poletti, G.; Sangregorio, C. Synthesis and characterization of polyethylenimine-based iron oxide composites as novel contrast agents for MRI. *MAGMA* **2009**, *22*, 77−87.
(26) Valero, E.; Fiorini, S.; Tambalo, S.; Busquier, H.; Callejas-Fernández, J.; Marzola, P.; Gálvez, N.; Domínguez-Vera, J. M. In vivo long-term magnetic resonance imaging activity of ferritin-based magnetic nanoparticles versus a standard contrast agent. *J. Med. Chem.* **2014**, *57*, 5686−92.
(27) Snow, G. B.; Patel, P.; Leemans, C. R.; Tiwari, R. Management of cervical lymph nodes in patients with head and neck cancer. *Eur. Arch Otorhinolaryngol.* **1992**, *249*, 187−94.
(28) Stokkel, M. P.; Moons, K. G.; ten Broek, F. W.; van Rijk, P. P.; Hordijk, G. J. 18F-fluorodeoxyglucose dual-head positron emission tomography as a procedure for detecting simultaneous primary tumors in cases of head and neck cancer. *Cancer* **1999**, *86*, 2370−7.
(29) Conti, P. S.; Lilien, D. L.; Hawley, K.; Keppler, J.; Grafton, S. T.; Bading, J. R. PET and [18F]-FDG in oncology: a clinical update. *Nucl. Med. Biol.* **1996**, *23*, 717−35.
(30) Joo, Y. H.; Yoo, I. R.; Cho, K. J.; Park, J. O.; Nam, I. C.; Kim, C. S.; Kim, S. Y.; Kim, M. S. The value of preoperative 18F-FDG PET/CT for the assessing contralateral neck in head and neck cancer patients with unilateral node metastasis (N1−3). *Clin Otolaryngol.* **2014**, *39*, 338−44.
(31) Mussa, A.; Sandrucci, S. *Nuove Tecnologie Chirurgiche in Oncologia*; Springer, 2011.

DOI: 10.1021/acsmedchemlett.7b00278
ACS Med. Chem. Lett. 2017, 8, 1230−1235